Characterization of hydrodynamic properties of a gas–liquid–solid three-phase fluidized bed with regular shape spherical glass bead particles

H.M. Jena [a], B.K. Sahoo [b], G.K. Roy [a], B.C. Meikap [b],*

[a] Department of Chemical Engineering, National Institute of Technology (NIT), Rourkela 769008, Orissa, India
[b] Department of Chemical Engineering, Indian Institute of Technology (IIT), P.O. Kharagpur Technology, Kharagpur 721302, West Bengal, India

ABSTRACT

The hydrodynamic characteristics, viz., the pressure drop, bed expansion and phase hold-up of a co-current gas–liquid–solid three-phase fluidized bed has been studied using liquid as the continuous phase and gas as the discontinuous phase. These have been done in order to develop a good understanding of each flow regime in gas–liquid and liquid–solid fluidization. Air, water and glass beads (2.18, 3.05 and 4.05 mm, respectively) are used as the gas, liquid and solid phases, respectively. The experiments were carried out in a 100 mm ID, 2 m-height vertical Plexiglas column. The column consists of three sections, viz., the gas–liquid disengagement section, test section and gas–liquid distributor section. Bed pressure measurements have been made to predict the minimum liquid fluidization velocity. By keeping gas velocity at a fixed value, the liquid velocity was varied and the effect on phase hold-up, minimum liquid fluidization velocity, pressure drop and the expansion ratio was studied for different particle size and static bed height. Experimental study based on statistical design has been made to investigate the expansion ratio of fluidized bed and a correlation has been developed for gas hold-up. It is evident from the correlation that gas hold-up is strongly function of modified gas Reynolds number and independent of liquid Reynolds number. The experimental values have been compared with those predicted by the correlations and have been found to agree well.

© 2008 Elsevier B.V. All rights reserved.

1. Introduction

Gas–liquid–solid fluidization also known as three-phase fluidization is a subject of fundamental research since the last three decades due to its industrial importance. Three-phase fluidized beds have been applied successfully to many industrial processes such as in the H-oil process for hydrogenation and hydro-desulfurization of residual oil, the H-coal process for coal liquefaction, Fischer–Tropsch process, and the bio-oxidation process for wastewater treatment.

Three-phase fluidized beds are also often used in physical operations [1]. As in the case of fixed bed operation, both co-current and countercurrent gas–liquid flow are permissible, and for each of these both bubble flows, in which the liquid is the continuous phase and the gas dispersed, and trickle flow. In which the gas forms a continuous phase and the liquid is more or less dispersed [2]. Gas–liquid–solid fluidization can be classified mainly into four modes of operation. These modes are co-current three-phase fluidization with liquid as the continuous phase (mode Ia); co-current

three-phase fluidization with gas as the continuous phase (mode-Ib); inverse three-phase fluidization (mode IIa); and fluidization represented by a turbulent contact absorber (TCA) (mode IIb). Modes IIa, and IIb are achieved with a countercurrent flow of gas and liquid. Amongst which the most striking one is the co-current three-phase fluidization with the liquid as the continuous phase [1]. The co-current gas–liquid–solid fluidization is defined as an operation in which a bed of solid particles is suspended in gas and/or liquid upward flowing media due to the net gravitational force on particles. Such an operation generates considerable intimate contact among the gas, liquid and solid particles in these systems and provides substantial advantages for applications in physical, Chemical or biochemical processing involving gas, liquid and solid phases [3].

The successful design and operation of a gas–liquid–solid fluidized bed system depends on the ability to accurately predict the fundamental characteristics of the system. Specially, the hydrodynamics, the mixing of individual phases, and the heat and mass transfer characteristics [4,5]. Knowledge of minimum liquid fluidization velocity is essential for the successful operation of gas–liquid–solid fluidized beds. For gas–liquid–solid fluidized systems the minimum liquid fluidization velocity is the superficial liquid velocity at which the bed becomes fluidized for a given gas superficial velocity [6]. The minimum liquid flow rates required to

* Corresponding author. Tel.: +91 3222 283958; fax: +91 3222 282250.
E-mail addresses: hara_jena@rediffmail.com (H.M. Jena),
bcmeikap@che.iitkgp.ernet.in (B.C. Meikap).

Nomenclature

A	cross-sectional area of the column (m^2)
d_p	particle diameter (mm)
H	average height of expanded bed (m)
H_s	static bed height (m)
M_s	mass of the solid in the bed (kg)
ΔP	pressure drop (Pa)
Re_l	liquid Reynolds number
Re_g	modified gas Reynolds number
V_l	liquid velocity (m/s)
V_g	gas velocity (m/s)
V_{lmf}	minimum liquid velocity for a three-phase system (m/s)
V_{imf}^{ls}	minimum liquid fluidization velocity for liquid–solid system (m/s)

Greek letters

β_u	ratio of superficial velocities $=(V_g/V_l)$
$\varepsilon_g, \varepsilon_l, \varepsilon_s$	gas, liquid and solids hold-ups
μ	phase viscosity (Ns/m^2)
ρ_g, ρ_l, ρ_s	gas, liquid and particle density (kg/m^3)

achieve fluidization are determined by a plot of the pressure drop across the bed versus the superficial liquid velocity at constant gas flow rate. During fluidization the pressure drop across the bed will no longer change with increasing liquid flow rate. Thus the flow rates at which a break in curve occurs correspond to the minimum fluidization velocities [4]. Visual observations determine the liquid minimum fluidization velocity as either the velocity at which the bed first begins to expand or as the velocity at which any particle with in the bed continuously shifts position with neighboring particles [7].
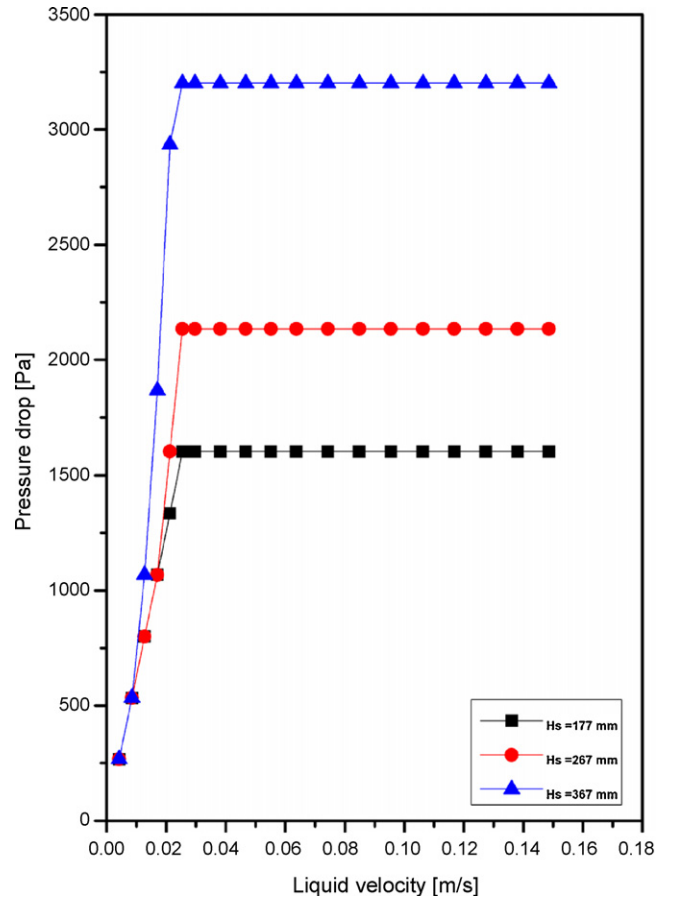

Fig. 2. Variation of pressure drop with liquid velocity for different bed height at V_g =0 m/s for 2.18 mm glass beads.
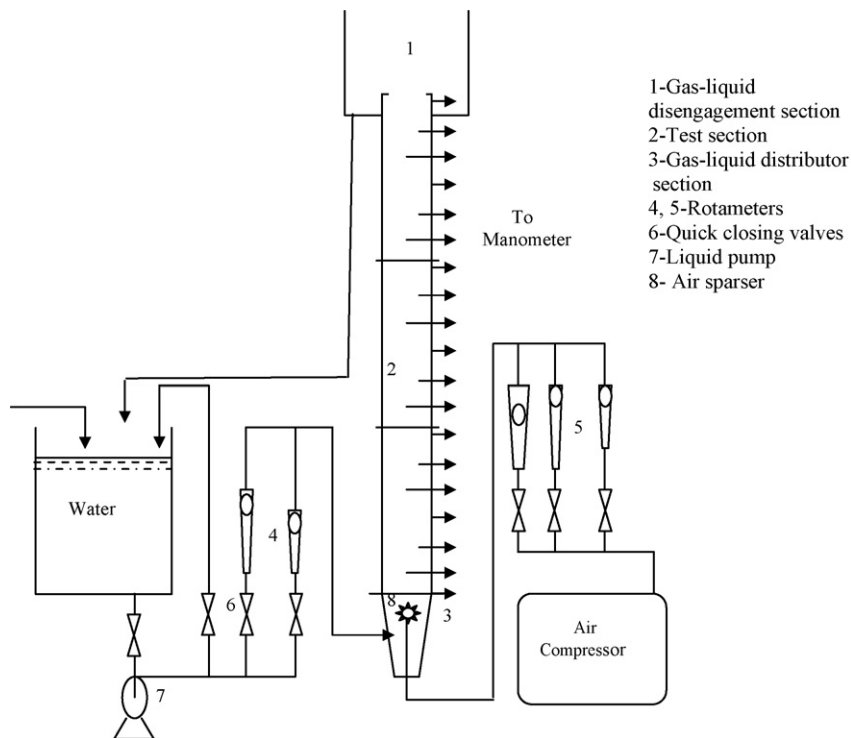

Fig. 1. Schematic diagram of the three-phase fluidized bed.

Table 1
Properties of bed materials (A), fluidizing medium (B), manometric fluid (C)

Particle notation	Materials	Mesh size	d_p (mm)	ρ_p (kg/m^3)
(A) Properties of bed materials				
P1	Glass beads	−7 + 8	2.18	2216
P2	Glass beads	−5 + 6	3.05	2253
P3	Glass beads	−4 + 5	4.05	2470
Fluidizing medium			ρ (kg/m^3)	μ (Ns/m^2)
(B) Properties of fluidizing medium				
Air at 25 °C			1.168	0.00187
Water at 25 °C			1.000	0.095
Manometric fluid			ρ (kg/m^3)	μ (Ns/m^2)
(C) Properties of manometric fluid				
Mercury			13600	0.15
Carbon tetra-chloride (CCl$_4$)			1590	0.09

For chemical processes where mass transfer is the rate-limiting step, it is important to be able to estimate the gas hold-up as this relates directly to the mass transfer [8–10]. The following equations have typically been used to determine the volume fraction (hold-up) of each phase in the three-phase fluidized bed:

$$\varepsilon_g + \varepsilon_l + \varepsilon_s = 1 \tag{1}$$

$$\Delta P = gH(\rho_g \varepsilon_g + \rho_l \varepsilon_l + \rho_s \varepsilon_s) \tag{2}$$
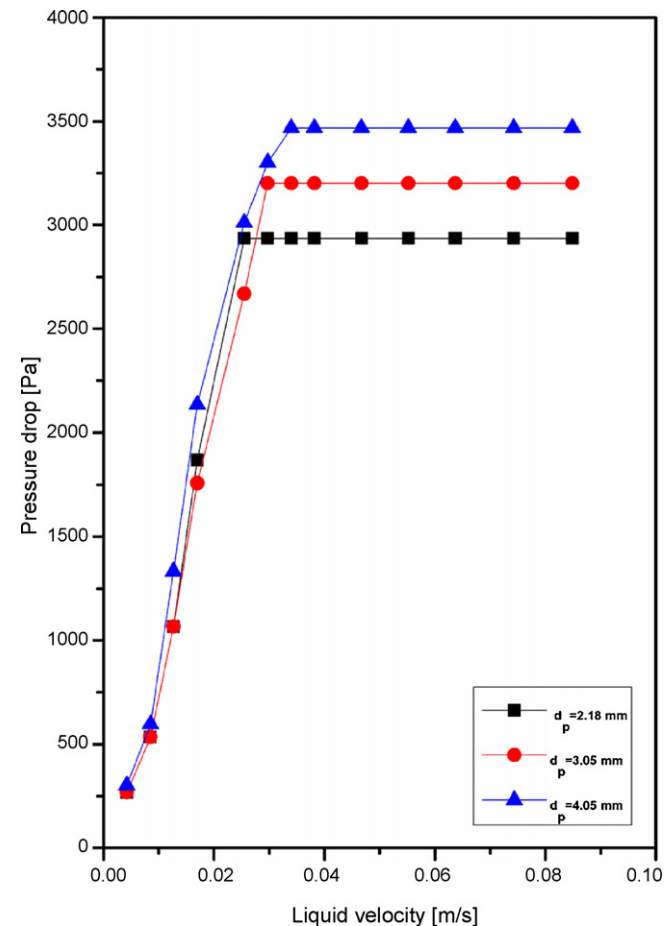
$$\varepsilon_s = \frac{M_s}{\rho_s AH}. \tag{3}$$

Where the bed height in Eqs. (2) and (3) is obtained either visually or from the measured pressure drop gradient [11]. A more direct method of measuring ε_g is to simply isolate a representative portion of the test section by simultaneously shutting two quick closing valves and measuring the fraction of the isolated volume occupied by the gas [2]. Other most promising methods of measuring the local gas hold-up are electroresistivity, electro conductivity methods, γ-ray transmission measurements and radioactive tracer techniques [2–4,12–16].

In the present study experiments were conducted to examine the hydrodynamic behavior, viz., the pressure drop, minimum fluidization, bed expansion and phase hold-up of a co-current gas–liquid–solid three-phase fluidized bed using liquid as the continuous phase and gas as the discontinuous phase. These have been done in order to develop a good understanding of each flow regime in gas–liquid and liquid–solid fluidization. Correlation based on factorial design analysis [14] has been developed for the bed expansion ratio and compared with the experimental values. Also a correlation derived from dimensional analysis has been proposed for gas hold-up and compared with the correlations of [8]. The novelty of the system is that it can be used for wastewater treatment containing hazardous chemicals.

2. Experimental

A schematic diagram of the experimental setup is shown in Fig. 1. The vertical Plexiglas fluidized bed reactor is of 100 mm ID with a maximum height of 2 m. The column consists of three sections, viz., the gas–liquid disengagement section, test section,
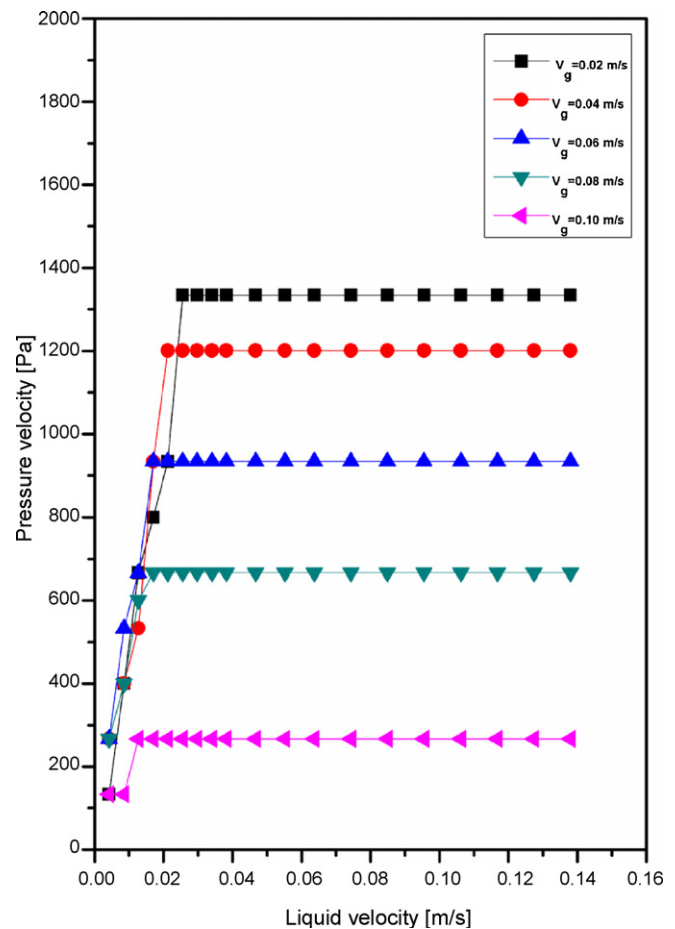

Fig. 3. Variation of pressure drop with liquid velocity for different particle size at V_g =0.02 m/s for H_s =367 mm.

Fig. 4. Variation of pressure drop with liquid velocity at different gas velocity for H_s =267 mm for 3.05 mm glass beads.

and gas–liquid distributor section. The gas–liquid distributor is located at the bottom of the test section and is designed in such a manner that uniform distribution of the liquid and gas can be maintained in the column. The distributor section is a conical frustum of 120 mm in height, one end 50.8 mm in diameter and the other end of 100 mm diameter having liquid inlets one of 240 mm ID with a perforated plate made of G.I. sheet of 1 mm thick, 120 mm diameter, of about 278 numbers of 2, 2.5 and 3 mm pores in placed at the top of this section. There is a gas distributor consists of 50 numbers of 1 mm pores placed randomly. In this section the gas and liquid streams merged and passed through the perforated grid. The mixing section and grid ensure that the gas and liquid are well mixed and evenly distributed into the bed. Gas–liquid disengagement section is at the top of the column, which allows gas to escape and liquid to be circulated. Any entrained particles retain on the screen attached to the top of this section. For pressure drop measurement the pressure ports are being fitted to the manometers of 1 m long (each limb) filled with mercury. The design is to measure the pressure drops at a particular section at three different locations such as at the wall, at the center of the column and at one fourth of the diameter of the column from the wall, so that the wall effects and the gas hold-up can be studied clearly.

The three phases (solid, liquid and gas) present in the column were 2.18, 3.05 and 4.05 mm glass beads, tap water and the oil free compressed air. The properties of the bed material, the fluidizing medium and the manometric fluid are shown in Table 1. The air–water flow were co-current and upwards. Accurately weighed amount of material was fed into the column and adjusted for a specified initial static bed height. Water was pumped to the fluidized

bed reactor at a desired flow rate. Then air was injected into the column through the air distributor. Approximately five minutes was allowed to make sure that the steady state was reached. Then the readings of each manometer were taken. Also, the bed expansion was noted. For gas hold-up measurement, the water and air rotameters valves were quickly closed at same proportion. The values of minimum fluidization velocity for every run have been obtained by plotting pressure drop across the beds versus liquid flow rates at constant air flow rates. The same procedure was repeated for different materials at different static bed height.

3. Results and discussion

3.1. Pressure drop and minimum fluidization velocity

The minimum fluidization velocity in this study was obtained from the relationship between pressure gradient and superficial liquid velocity. Figs. 2 and 3 show the variation of pressure drop with superficial liquid velocity for liquid–solid system at various bed heights and particle size. From this it is observed that bed mass has no effect on minimum fluidization velocity, but minimum fluidization velocity increases with increase in particle, which is listed in Table 2.

Fig. 4 shows the variation of pressure drop with superficial liquid velocity for gas–liquid–solid system for different superficial gas velocities. The minimum fluidization velocity decreases with increase in gas velocity. The minimum fluidization velocity decreases with increase in gas velocity is due to the increase in gas
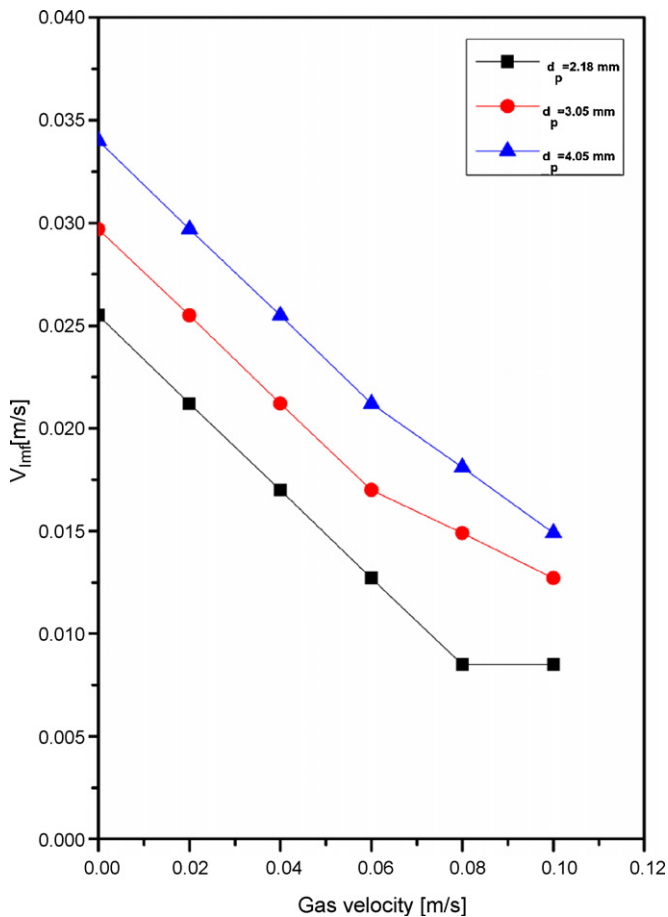

Fig. 5. Variation of minimum liquid fluidization velocity with gas velocity for different particle size at constant static bed height.
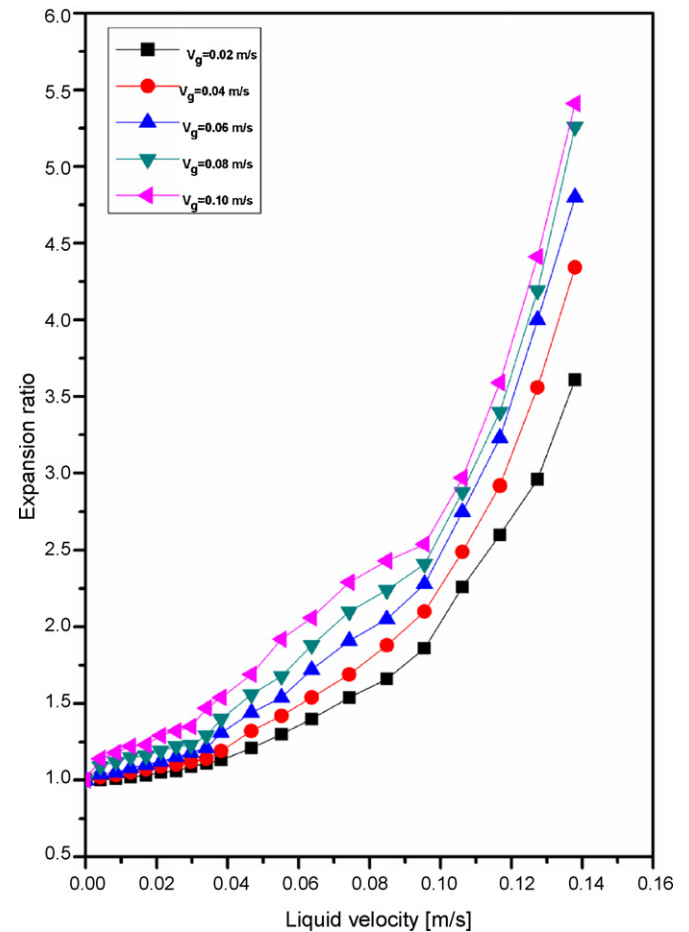

Fig. 6. Variation of expansion ratio with liquid velocity at different gas velocity at H_s =267 mm for 3.05 mm glass beads.

Table 2
Comparison of minimum fluidization velocity for different particle size at different gas velocities

d_p (mm)	V_{lmf} for					
	$V_g = 0$ m/s	$V_g = 0.02$ m/s	$V_g = 0.04$ m/s	$V_g = 0.06$ m/s	$V_g = 0.08$ m/s	$V_g = 0.10$ m/s
2.18	0.0255	0.0212	0.0170	0.0127	0.0085	0.0085
3.05	0.0297	0.0255	0.0212	0.0170	0.0149	0.0127
4.05	0.0340	0.0297	0.0255	0.0212	0.0181	0.0149

Table 3
Scope of the factors for hydrodynamics

Serial no.	Name of the variables	Factorial variables (general symbol)	Factorial design symbol	Maximum level (−1)	Minimum level (+1)	Magnitude of variables
1	Static bed height (mm)	H_s	A	177	367	177, 267, 367
2	Particle diameter (mm)	d_p	B	2.18	4.05	2.18, 3.05, 4.05
3	Gas velocity (m/s)	V_g	C	0.02	0.10	0.02, 0.04, 0.06, 0.08, 0.10

velocity tend to increase the hold-up and density reduces for whole mixture. Fig. 5 shows the variation of minimum fluidization velocity with superficial gas velocity for different particle size. Minimum fluidization velocity decreases with gas velocity, but more for particles of higher sizes. Finally, a comparison of minimum fluidization velocity is listed in Table 2.

3.2. Bed expansion

The bed voidage increases with both increasing liquid velocity and gas velocity as shown in Fig. 6. Correlation based on factorial design analysis [14] has been developed for the bed expan-
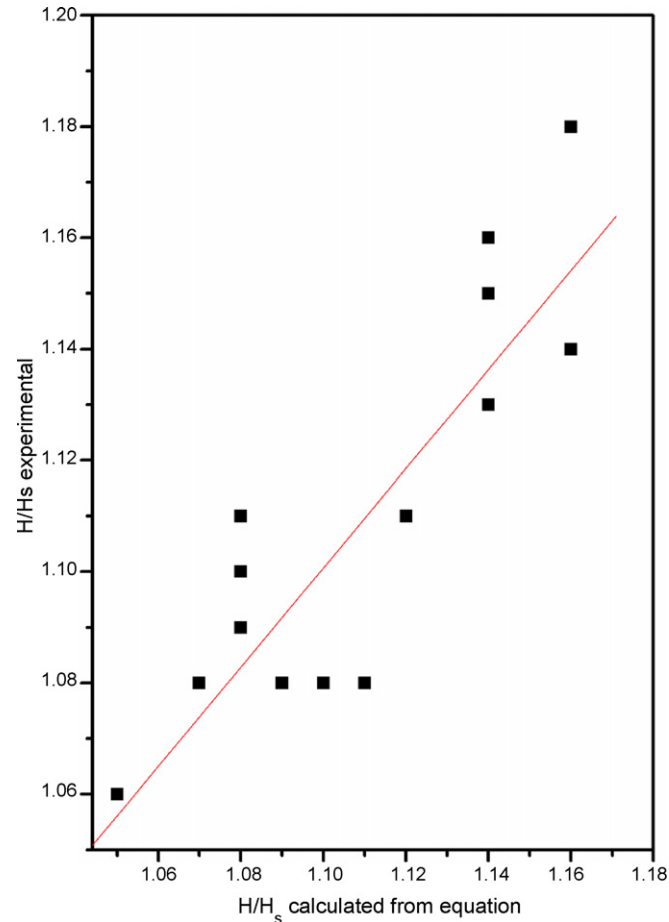
sion ratio. The method of factorial design analysis bring out the interaction effects of variables, which would not be found otherwise by conventional experimentation and to explicitly find out the effect of each of the variables quantitatively on the response.

The scope of the factors consider for factorial experimentation is presented in Table 3. The variables which affect bed expansion ratios in fluidization are static bed height, particle diameter and gas velocity. Thus total numbers of experiments required at two levels for the three variables is eight for responses expansion ratio at minimum fluidization velocity.
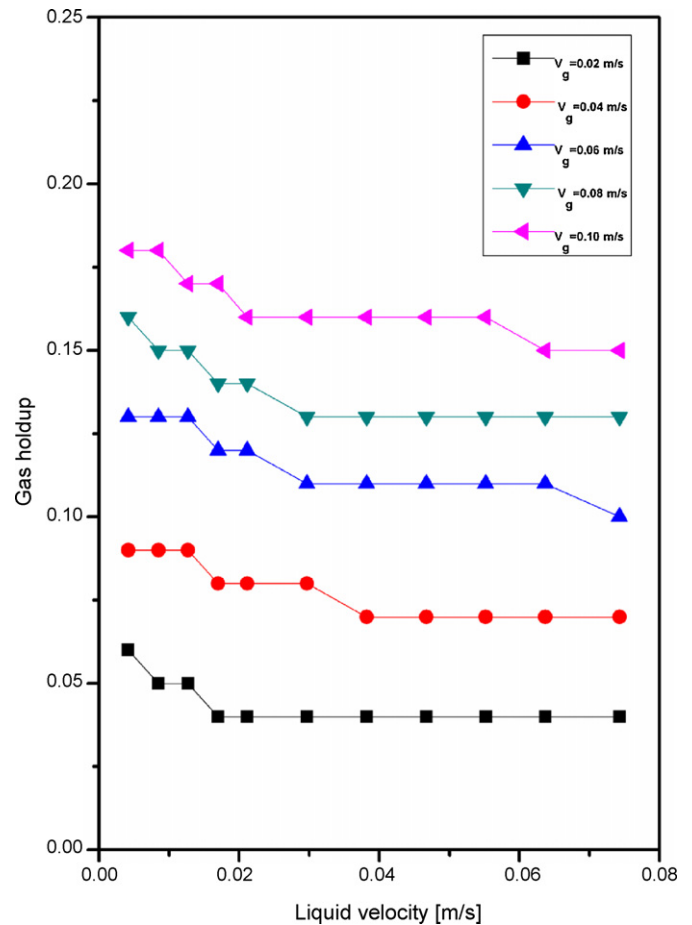

Fig. 7. Comparison of experimental values of expansion ratio with those calculated by Eq. (5).

Fig. 8. Variation of gas hold-up with liquid velocity at different gas velocity at $H_s = 267$ mm for 2.18 mm glass beads.

3.2.1. Development of model equation

The model equations are assumed to be linear and the equations take the general form,

$$Y = (b_0 + b_1A + b_2B + b_3C + \cdots + b_{12}AB + b_{13}AC + \cdots + b_{123}ABC). \tag{4}$$

Coefficients are calculated by the Yates technique; $b_i = \sum(\alpha_i Y_i)/N$. The following equation has been obtained,

$$Y = (1.05 + 0.0225B - 0.0175C + 0.01AB + 0.01ABC). \tag{5}$$

The value of the coefficients indicates the magnitude of the effect of the variables and the sign of the coefficient gives the direction of the effect of the variable. That is a positive coefficient indicating an increasing in the value of the responses with increase in the value of the variable and a negative coefficient showing that the response decreases with increase in the value of the variable. The comparison of the experimental values with that of calculated values from Eq. (5) shows good agreement as shown in Fig. 7.

3.3. Gas hold-up

Figs. 8 and 9 show the variation of gas hold-up with liquid velocity at various fixed gas velocities and with gas velocity at different fixed liquid velocities. It is found that with increase in liquid velocity the gas hold-up decreases but remains constant after reaching a moderate value of liquid velocity, with increase in gas velocity at constant liquid velocity the gas hold-up increases monotonically.
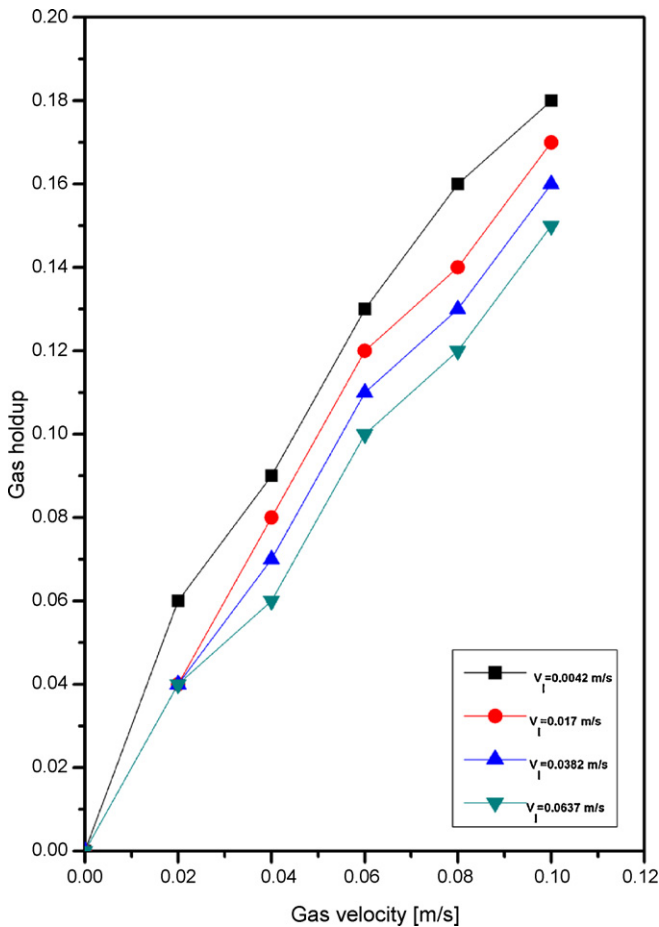

Fig. 9. Variation of gas hold-up with gas velocity at different liquid velocity at H_s =267 mm for 2.18 mm glass beads.
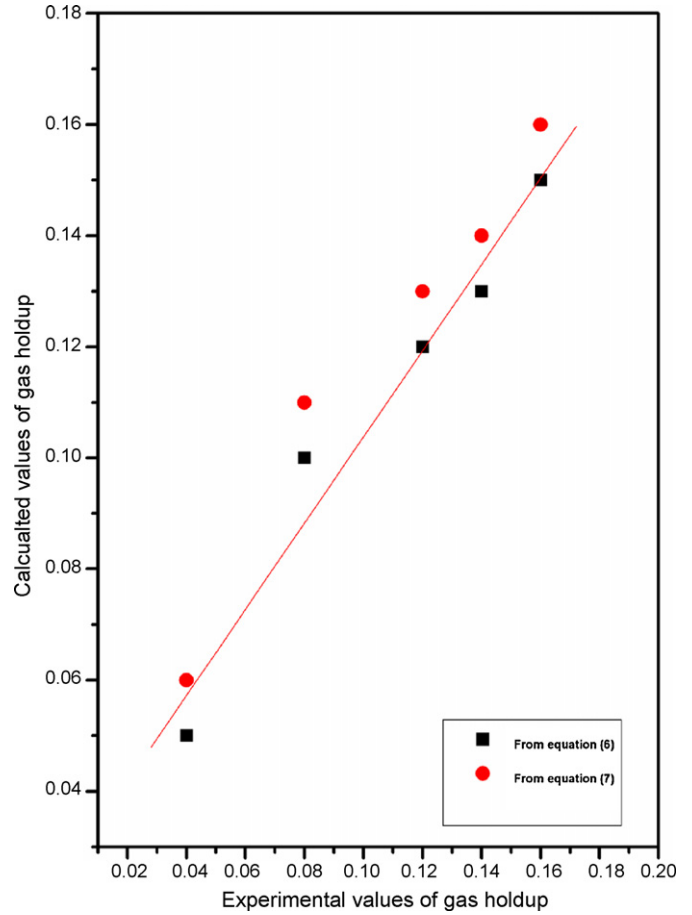

Fig. 10. Comparison of experimental values of gas hold-up with those calculated from Eqs. (6) and (7).

The average gas hold-up was plotted against modified gas Reynolds number (Re_g) for $12.64 \le Re_l \le 309.60$. The results were fitted to a power-law equation passing through the origin (at zero gas flow rate) as,

$$\varepsilon_g = 0.0023Re_g^{0.73} \tag{6}$$

The Safoniuk et al. [8] correlation is given by,

$$\varepsilon_g = 0.0139Re_g^{0.426}. \tag{7}$$

Fig. 10 shows the comparison of experimental values of gas hold-up with those calculated from Eqs. (6) and (7). Higher hold-up is seen for Eq. (7).

4. Conclusions

The hydrodynamic study of the three-phase fluidized bed reveals that the minimum liquid fluidization velocity (V_{lmf}) increases with increase in particle size at constant gas velocity but decreases with increase in gas velocity at constant liquid velocity. The expansion ratio increases with increase in liquid and gas velocity and decreases with increase in particle size and static bed height. The gas hold-up increases monotonically when the gas velocity is increased. At a fixed gas velocity, at low liquid velocity gas hold-up decreases and remains constant with further increase in liquid velocity. Gas hold-up increases with increase in particle size. It is evident from the correlation that gas hold-up is a strong function of modified gas Reynolds number and independent of liquid Reynolds number.

References

[1] K. Muroyama, L.S. Fan, Fundamentals of gas–liquid–solid fluidization, AIChE. J. 3 (1985) 1–34.

[2] N. Epstein, Three-phase fluidization: some knowledge gaps, Can. J. Chem. Eng. 59 (1981) 649–757.

[3] V.R. Dhanuka, J.B. Stepanek, Gas and Liquid Hold-up and Pressure Drop Measurements in a Three-Phase Fluidized Bed, Fluidization, University Press, Cambridge, 1978, pp. 179–183.

[4] J.M. Begovich, J.S. Watson, Hydrodynamic Characteristics of Three-Phase Fluidized Beds, Fluidization, University Press, Cambridge, 1978, pp. 190–195.

[5] T.J. Lin, C.H. Tzu, Effects of macroscopic hydrodynamics on heat transfer in a three-phase fluidized bed, Catal. Today 79–80 (2003) 159–167.

[6] L.A. Briens, C.L. Briens, A. Margaritis, J. Hay, Minimum liquid fluidization velocity in gas–liquid–solid fluidized beds, AIChE. J. 43 (1997) 1180–1189.

[7] L.A. Briens, C.L. Briens, A. Margaritis, J. Hay, Minimum liquid fluidization velocity in gas–liquid–solid fluidized beds of low-density particles, Chem. Eng. Sci. 52 (1997) 4231–4238.

[8] M. Safoniuk, J.R. Grace, L. Hackman, C.A. Mcknight, Gas hold-up in a three-phase fluidized bed, AIChE. J. 48 (2002) 1581–1587.

[9] J.M. Schweitzer, J. Bayle, T. Gauthier, Local gas hold-up measurements in fluidized bed and slurry bubble column, Chem. Eng. Sci. 56 (2001) 1103–1110.

[10] L.S. Fan, F. Bavarian, R.I. Gorowara, B.E. Kreischer, Hydrodynamics of gas–liquid–solid fluidization under high gas hold-up conditions, Powder Technol. 53 (1987) 285–293.

[11] S.P. Kim, C.G.J. Baker, M.A. Bergougnou, Phase holdup characteristics of three-phase fluidized beds, Can. J. Chem. Eng. 53 (1975) 134–139.

[12] V.K. Bhatia, N. Epstein, Proc. Int. Symp. on Fluidization and its Applications, Toulouse, 1974, p. 380.

[13] H. Yu, B.E. Rittman, Predicting bed expansion and phase hold-up for three-phase fluidized bed reactors with and without bio-film, Water Res. 31 (10) (1997) 2604.

[14] O.L. Davies, Design and Analysis of Industrial Experiments, 2nd ed., Longman Publishers, New York, 1978.

[15] S.A. Razzak, S. Barghi, J.-X. Zhu, Electrical resistance tomography for flow characterization of a gas–liquid–solid three-phase circulating fluidized bed, Chem. Eng. Sci. 62 (2007) 7253–7263.

[16] G. Jin, Multi-scale modeling of gas–liquid–solid three-phase fluidized beds using the EMMS method, Chem. Eng. J. 117 (2006) 1–11.